Preprints of the 21st IFAC World Congress (Virtual)
Berlin, Germany, July 12-17, 2020

Robust Controller Design for Feedback Architectures with Signal Shapers

Martin Goubej *, **Miloš Schlegel** * **Tomáš Vyhlídal** **

* *NTIS Research Centre, University of West Bohemia, Technická 14, 306 14 Pilsen, Czechia, e-mail: mgoubej@ntis.zcu.cz, schlegel@ntis.zcu.cz*
** *Department of Instrumentation and Control Engineering, and Center of Advanced Aerospace Technology, Faculty of Mechanical Engineering, Czech Technical University in Prague, Czechia, e-mail: tomas.vyhlidal@fs.cvut.cz*

Abstract: Available feedback architectures with time delay based signal shapers are outlined and studied with the objective to determine the channels in which the flexible mode compensation (by the shaper) takes place. As the main result, a systematic methodology for the robust controller design is proposed and tested for three most common feedback architectures with signal shapers. The validation is performed on a Gantry crane anti-sway problem, considering four types of distributed delay shapers. It is demonstrated that for the selected robustness H_∞ measure, the applicable parameter range is considerably reduced by placing the signal shaper to the loop. Still, the obtained characteristics and responses of shaper feedback architectures show that viable controller setting can well be found by the considered control design method.

Keywords: Input shaper, H_∞ norm, robust control design, time delay system

1. INTRODUCTION

Following the pioneering work by Smith (1958), input shaping by time delay filters has become an established technique to pre-compensate oscillatory modes of flexible systems. The first results on Smith's shaper (known as *posicast*) were followed by Singer and Seering (1990); Singhose et al. (1994) and other successors. A typical application of input shaping is the pre-comensation of flexible modes in crane systems, see e.g. Vaughan et al. (2010); Singhose et al. (2008). An extensive review on input shaping was reported by Singhose (2009).

Recently, alternative shaper forms with distributed delay were proposed. In Vyhlídal et al. (2013), zero-vibration shaper with equally distributed delay was proposed. The structure of distributed delay shaper was relaxed by Vyhlídal and Hromčík (2015) and the shaper parametrization was turned from numeric to analytic form. Next to smoothing the response at its settling stage, the positive feature of distributed delay shapers are retarded spectra of zeros. This spectral property is advantageous if the shapers are embedded within feedback loops, Vyhlídal et al. (2016). Inclusion of the shaper to the feedback loop is motivated by pre-compensation of the flexible modes in responses induced by various disturbances, Smith (1958), Hung (2003), Huey et al. (2008). The second motivation for placing the shaper to a feedback loop is in handling the effect of non-linearities, mainly the control input saturation, Huey et al. (2008), Alikoç et al. (2017). However, once the shaper with time delays is included to the feedback loop, the closed loop system becomes infinite dimensional system. Designing a finite-order controller for such a feedback is not a straightforward task. The first attempts in this direction, Vyhlídal et al. (2016), Pilbauer et al. (2017), Pilbauer et al. (2018), are further elaborated in this paper, which is structured as follows. The purpose and applicability of three feedback structures with shapers are outlined in Section 2. The Section 3 then presents the main result - the methodology on robust fixed structure controller design. The proposed method is validated in Section 4 on a typical case study example - Gentry crane anti-sway problem. The main results are summarised in Section 5.

2. SURVEY ON FEEDBACK INTERCONNECTIONS WITH INPUT SHAPER

Three feedback configurations with shaper shown in Fig. 1-3 are considered. The controlled plant consists of two subsystems. The first subsystem $G(s)$ describes an actuator dynamics which is a part of the velocity or position feedback loop together with the controller $C(s)$. The second subsystem $F(s)$ contains oscillatory mode determined by the damping ξ and natural frequency ω, which is to be targeted by the shaper.

The standard objective is to design the motion control system in such a way that the flexible dynamics in $F(s)$ does not get excited due to the changing the reference w. As will be shown, some of the schemes achieve the mode compensation also to responses induced by measurement noise n and output disturbance d. Note that also an input disturbance acting on $G(s)$ may be considered but it can be transformed to an equivalent output signal d without a loss of generality. Let us also note that it is assumed that there is no back propagation of the output y_s back to the feedback loop. This assumption is quite

common for motion systems with clearly separable rigid and oscillatory dynamics and negligible interactions in the load to actuator direction, Vyhlídal et al. (2016).

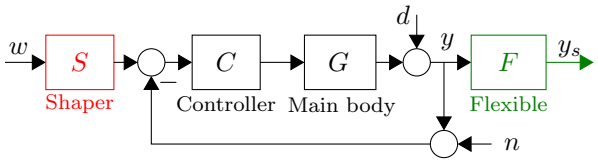

Fig. 1. *Feedforward shaper* application

A common way to suppress the unwanted load-side oscillations is to employ a signal shaper $S(s)$ to modify the reference setpoint for the feedback loop (Fig. 1). The advantage is that the shaper and feedback control parts can be designed independently and the shaper dynamics does not influence performance nor stability of the loop. By analyzing the transfer function from the reference to load-side output, we get

$$T_{w,y}(s) = \frac{Y(s)}{W(s)} = F(s)S(s)\frac{C(s)G(s)}{1+C(s)G(s)}, \qquad (1)$$

from which one may see that the vibration due to the reference w are canceled provided that the shaper zeros match the oscillatory poles of $F(s)$. On the other hand, the remaining disturbance sources are not compensated and they still excite the oscillatory dynamics, which can be observed from the respective transfer functions

$$\begin{aligned} T_{n,y}(s) &= \frac{Y(s)}{N(s)} = -F(s)\frac{C(s)G(s)}{1+C(s)G(s)}, \\ S_{d,y}(s) &= \frac{Y(s)}{D(s)} = F(s)\frac{1}{1+C(s)G(s)}. \end{aligned} \qquad (2)$$

The oscillatory poles of $F(s)$ get excited unless there is a cancellation with open-loop poles or zeros in eq. (2).

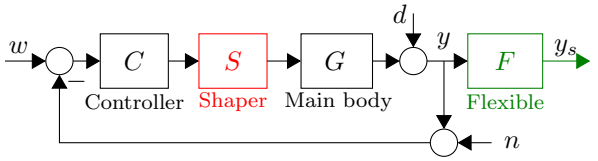

Fig. 2. Feedback loop with *control-action shaper*

Secondly, we consider the scheme with *control-action shaper* shown in Fig. 2, in which the signal shaper gets embedded directly in the feedback loop. The given scheme was studied by Hung (2003) with a link to Smith's Posicast. Stability aspects were then analysed by Staehlin and Singh (2003) and by Huey and Singhose (2009). Checking the corresponding dynamics from all the external signals yields

$$\begin{aligned} T_{w,y}(s) &= \frac{Y(s)}{W(s)} = F(s)\frac{C(s)S(s)G(s)}{1+C(s)S(s)G(s)}, \\ T_{n,y}(s) &= \frac{Y(s)}{N(s)} = -F(s)\frac{C(s)S(s)G(s)}{1+C(s)S(s)G(s)}, \\ S_{d,y}(s) &= \frac{Y(s)}{D(s)} = F(s)\frac{1}{1+C(s)S(s)G(s)}. \end{aligned} \qquad (3)$$

It is seen that the load-side oscillations are not excited from the reference nor the measurement noise, reported by Huey et al. (2008), but still the input or output disturbance will cause unwanted resonance response.

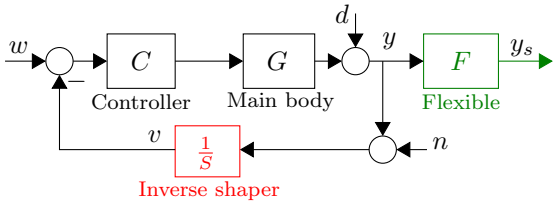

Fig. 3. Feedback loop with *inverse shaper*, Vyhlídal et al. (2016)

The last structure under consideration is the scheme shown in Fig. 3 with an *inverse shaper*. In this case, an inverse implementation of the signal shaper $1/S$ is used in the feedback path. The *inverse shaper* scheme proposed by Vyhlídal et al. (2016) can be considered as a more efficient alternative of the compensator-based feedback scheme proposed already by Smith (1958). Both the Smith's and Vyhlidal's schemes were designed with the aim to achieve the flexible mode compensation in output (and input) disturbance rejection responses.

Expressing the dynamics at the load-side output due to the set-point and external disturbances lead to

$$\begin{aligned} T_{w,y}(s) &= \frac{Y(s)}{W(s)} = F(s)\frac{C(s)S(s)G(s)}{S(s)+C(s)S(s)G(s)}, \\ T_{n,y}(s) &= \frac{Y(s)}{N(s)} = -F(s)\frac{C(s)G(s)}{S(s)+C(s)S(s)G(s)}, \\ S_{d,y}(s) &= \frac{Y(s)}{D(s)} = F(s)\frac{S(s)}{S(s)+C(s)S(s)G(s)}. \end{aligned} \qquad (4)$$

This structure is able to compensate the load-side vibrations due to w and d but the feedback noise n excites the oscillatory dynamics of $F(s)$. Note that in Hromčík and Vyhlídal (2017), Pilbauer et al. (2018), the inverse shaper design was proposed for the coupled dynamics of the main body and flexible subsystem.

The shaper $S(s)$ is commonly designed as a time delay filter with a non-negative impulse response which projects to non-decreasing character of the set-point response. Time delays related to oscillation period also bring a natural control-signal phasing in both the set-point and disturbance rejection responses. Thus the shaper has potential to contribute to energetic-optimality of the control actions. On the other hand, the shaper time-delays within the feedback loop complicate analysis and synthesis of the feedback controller $C(s)$ due to the infinite order of the resulting dynamics. Conventional design methods working in the algebraic domain are difficult to employ due to the infinite number of poles. This disadvantage is mitigated in the frequency domain to some extent but still some partial steps of the design process, e.g. check of closed-loop stability, get complicated significantly. In what follows, a systematic methodology for the design of the feedback controller in the structures with embedded signal shapers according to Fig. 1- 3 is proposed and validated on a case study application.

3. FIXED-STRUCTURE ROBUST CONTROLLER DESIGN

We assume that a fixed-structure low-order controller $C(s)$, e.g. a PD, PI(D) or lead-lag compensator defined

by a set of two or three parameters, is to be designed and implemented. For this sake, we employ an algorithm based on recent results in H-infinity loop-shaping theory by the authors, Schlegel and Medvecová (2018) and Goubej and Schlegel (2019). For the sake of compactness, the proposed H_∞-region approach is briefly outlined here. The reader is referred to the respective publications for a more thorough explanation and derivation of the algorithm.

The starting point is an LTI plant model of the open-loop system to be controlled

$$P_1(s) = S(s)G(s), P_2(s) = \frac{G(s)}{S(s)}, \tag{5}$$

where $G(s)$ denotes the actuator-side dynamics and $S(s)$ is the direct- or inverse-form shaping filter embedded in the assumed control schemes from Fig. 2 and 3.

The goal is to find a feedback controller $C(s)$ which internally stabilizes the plant $P_i(s)$ and fulfills a set of design requirements formulated in the frequency domain as loop-shaping inequalities

$$||H(s,k)||_\infty < \gamma, \tag{6}$$

where H corresponds to an arbitrarily chosen closed-loop transfer function defined as a frequency-weighted transfer function between a chosen penalized output and generalized input

$$H(s,k) \triangleq W(s)S_*(s), \tag{7}$$

with $S_*(s)$ denoting one of the closed-loop sensitivity functions (e.g. the sensitivity, complementary-, input- and controller-sensitivity) and $W(s)$ introduces the user-defined frequency-dependent scaling.

Each of the design constraints can be transformed to the parametric space of the fixed-structure compensator. In case there are two controller gains to be tuned, the result of this transform defines a set of admissible controllers in the 2D plane. Full derivation of this transform was given in Schlegel and Medvecová (2018) for the particular case of PI controller. It was shown that the boundary of each H_∞ region can be computed by analyzing roots of a quadratic polynomial whose coefficients are linked with the transfer function of the controlled plant. Multiple design constraints can be combined by analyzing an intersection of their corresponding H_∞ regions. The resulting set of admissible controllers is then obtained as the intersection of all the H_∞ regions. In case it is non-empty, a particular controller may be obtained by forming a secondary performance criterion. An example of such secondary objective which is often used for the PI controller ($C(s) = K_p + K_i/s$) is the maximum integral gain condition which is known to minimize the Integral error criterion

$$IE = \int_0^{+\infty} e(t)\mathrm{d}t = \frac{1}{K_i}. \tag{8}$$

The H_∞ regions method can be applied directly to the formulated design problem of a motion system. It is assumed that the location of the flexible mode of $F(s)$ is known and a proper input shaper $S(s)$ is designed in the first step, either in the direct or inverse form according to the given feedback structures. Therefore, the controller $C(s)$ can be derived for the modified plant given by (5). The advantage is that the admissible regions in the parametric space of the fixed structure controller can be obtained in the same manner even for an infinite-order system which is formed by embedding a time-delay signal shaper in the loop. Moreover, the shape of the H_∞ regions resulting from the individual design constraints can give an important insight to the problem. The user can see which requirements are contradictory and how the insertion of the shaper in the loop affects the admissible set of controllers and therefore influence the achievable closed-loop performance and stability.

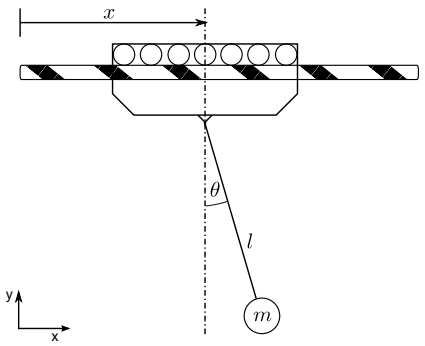

Fig. 4. Gantry crane anti-sway problem

The proposed methodology is summarized in Algorithm 1:

Algorithm 1 H_∞ loop-shaping controller design

Input: Plant model $G(s)$,$F(s)$
Output: Fixed-structure controller $C(s)$, shaping filter $S(s)$

1: Design the signal shaper $S(s)$ based on the flexible modes model in $F(s)$
2: Construct the augmented plant $P_1(s)$ or $P_2(s)$ in (5) based on the chosen feedback structure
3: Formulate closed-loop design requirements for $C(s)$ via loop-shaping inequalities (6)
4: Compute the corresponding H_∞ regions
5: Find the intersection of all regions to derive admissible set of controllers
6: Choose particular controller from the admissible set based on a secondary performance criterion, e.g. (8)

4. CASE STUDY: GANTRY CRANE APPLICATION

A case study is given to demonstrate the proposed approach to the design of the signal shaper-based feedback structure. A hoist-crane control problem from Fig. 4 is considered which fits the generic control setup assumed in Fig. 1-3. The actuator-side dynamics $G(s)$ is represented by the closed velocity loop of the hoist drive, whereas the load-side part $F(s)$ comes from the inherently oscillatory dynamics of the suspended load. The goal is to design the position controller $C(s)$ which is assumed to be of a PD type compensator

$$C(s) = \frac{U(s)}{E(s)} = (K_p + K_d s),\ E(s) = \mathcal{L}\{e(t) \triangleq x^*(t) - x(t)\}, \tag{9}$$

where x^* stands for the position reference variable.

The actuator dynamics is given as

$$G(s) = \frac{X(s)}{V^*(s)} = \frac{K(s+a)\prod_{i=1}^{2}(s^2+2\xi_i\omega_i s+\omega_i^2)}{s\prod_{j=1}^{4}(s^2+2\xi_j\omega_i s+\omega_j^2)}, \quad (10)$$

where $X(s) = \mathcal{L}\{x(t)\}$ denotes the hoist position and $V^*(s) = \mathcal{L}\{v^*(t)\}$ is a velocity setpoint. The model parameters were obtained from an experimental identification of a small-scale crane setup used at authors' department: $K = -13775$, $a = -149.2$, $\omega_i = \{154, 201\}s^{-1}$, $\xi_i = \{0.55, 0.059\}$, $\omega_j = \{38.1, 98, 155, 163\}s^{-1}$, $\xi_j = \{0.92, 0.57, 0.3, 0.07\}$. This part governs the dynamics of the hoist actuated by an AC induction motor including closed current and velocity control loops implemented in a frequency inverter unit. The load-side dynamics describing the transfer from hoist position to load sway angle is given as follows:

$$F(s) = \frac{\Theta(s)}{X(s)} = \frac{-3.06s^2}{s^2+0.087s+30.1} \quad (11)$$

with the mode determined by $\xi = 0.008$ and $\omega = 5.49s^{-1}$ to be targeted by the shaper. The parameters were obtained experimentally from the physical setup as well. The goal is to design the controller $C(s)$ from (9) for the three different shaping filter architectures introduced in Fig. 1-3.

Following shaper types were considered for comparison:

(1) *Distributed-delay Zero-vibration shapers* with the transfer function given in the form of

$$S_i(s) = A + (1-A)G_i(s)e^{-\tau s}, \; i = 1..4 \quad (12)$$

where $G_i(s)$ is a dynamics related to the filter delay distribution. Four distinct filter structures proposed in Vyhlídal and Hromčík (2015) were examined:

- DeZV shaper with equally distributed delay
$$G_1(s) = \frac{1-e^{-sT}}{sT}$$
- DtZV shaper with triangular delay distribution
$$G_2(s) = \frac{4(1-2e^{-sT/2}+e^{-sT})}{s^2T^2}$$
- DcZV shaper with trigonometric distribution
$$G_3(s) = \frac{4\pi^2(1-e^{-sT})}{sT(s^2T^2+4\pi^2)}$$
- DtaZV shaper with asymmetric triangular shape
$$G_4(s) = \frac{2(sT-1+e^{-sT})}{s^2T^2}$$

(2) *Conventional IIR single-mode notch-filter*

$$S_5(s) = \frac{s^2+2\xi\omega s+\omega^2}{s^2+2\omega s+\omega^2} \quad (13)$$

Let us note that shapers with distributed delay are selected to prevent undesirable *neutrality* of the closed loop which is likely to happen for classical lumped delay shapers, Vyhlídal et al. (2016).

The shapers were tuned to match the resonance of the oscillatory part of the system in (11) by setting $T = \frac{\pi}{\omega} = 0.574s$. The design requirement for the controller $C(s)$ is imposed as a maximum closed-loop sensitivity constraint defining a desired robustness margin

$$||S_{fk}(s)||_\infty < M_S, \; k = 1..3, \quad (14)$$

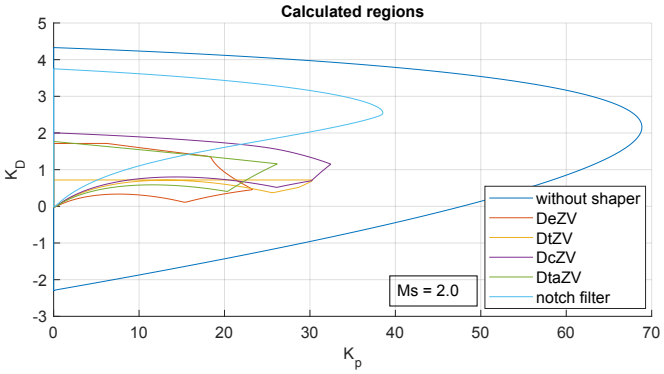

Fig. 5. Calculated H_∞ regions defining the sets of admissible PD controllers for the *inverse shaper* structure

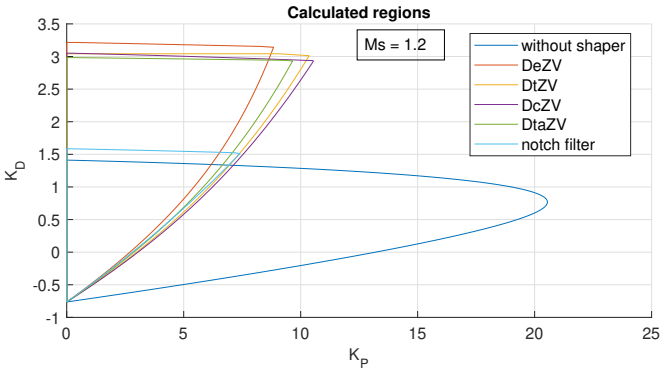

Fig. 6. Calculated H_∞ regions for the *control-action shaper* feedback structure

where $S_{fk}(s)$ corresponds to the three assumed control architectures from figures (1-3):

$$S_{f1} = \frac{1}{1+CG}, \; S_{f2} = \frac{1}{1+CSG}, \; S_{f3} = \frac{1}{1+CS^{-1}G}. \quad (15)$$

It may be observed that the formulated control design problem is equivalent to the synthesis of a PI controller $\bar{C}$ for a modified plant $\bar{G}$ as follows:

$$\bar{C}(s) \triangleq C(s)/s = K_d + \frac{K_p}{s} \triangleq \bar{K}_p + \frac{\bar{K}_i}{s}, \; \bar{G}(s) \triangleq G(s)s. \quad (16)$$

Therefore, previous results derived in (Schlegel and Medvecová, 2018) for the PI controller case can be applied directly for the pair $\bar{C}, \bar{G}$ and the PD controller in (9) for the original problem formulation is obtained from simple substitution of gains from (16). The maximum integral gain which minimizes the IE criterion (8) was chosen as a secondary objective for the selection of a particular controller from the derived admissible sets.

4.1 Achieved results

Figures 5 and 6 show the results of the computed H_∞ regions of the PD controller corresponding to the feedforward, control-action and inverse shaper structures from Figs. 1-3. The first observation is that the inclusion of the shaper in the loop significantly reduces the range of applicable gains which affects the achievable closed-loop bandwidth. The dynamics of the shaper has to be taken

Table 1. Derived parameters of S, C in direct $\{K_p^d, K_d^d\}$ and inverse $\{K_p^i, K_d^i\}$ structure

Filter type	τ	A	K_p^d	K_d^d	K_p^i	K_d^i
DeZV	0.286	0.395	8.841	3.142	23.3	0.465
DtZV	0.287	0.454	10.364	3.01	30.26	0.697
DcZV	0.287	0.465	10.542	2.93	32.42	1.15
DtaZV	0.39	0.436	9.656	2.93	26.13	1.16
notch	-	-	7.4	1.51	38.53	2.56
$S = 1$	-	-	20.55	0.77	-	-
$S = 1$	-	-	-	-	68.86	2.16

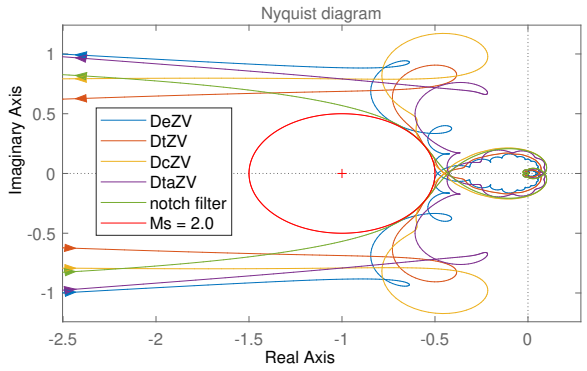

Fig. 7. Open-loop Nyquist plot for the inverse-shaper structure and optimal PD controllers ($K_p \to max$)

into consideration in the phase of feedback compensator design. Otherwise, the resulting performance may be inferior. The derived controller and shaper parameters are listed in Table 1.

Figure 7 shows the Nyquist plots for the optimal PD controllers chosen from the computed admissible regions as the points with the maximum proportional gain, according to the secondary objective in (8) and substitution in (16). The maximum sensitivity limit in the loop-shaping constraint (14) was set to be $M_S = 2$ for the inverse shaper structure and $M_S = 1.2$ for the control-action shaper case. It can be seen that the design requirement is met exactly, confirming correct functionality of the controller synthesis algorithm.

Figures 9 and 11 show the load-side response to the unit step reference position change. Comparable performance is observed for all the studied shaper types. However, a significant difference appears on the actuator-side position response shown in Fig. 8, which reveals much more oscillatory behavior when using the conventional notch-filter. This may advocate the employment of more complex distributed-delay shapers which are able to maintain almost monotonous actuator response.

Figures 10 and 12 demonstrate the load-side response to the step change in the output disturbance d. The control-action shaper cannot suppress the induced vibrations as shown in the previous section. The residual oscillations are even higher than in the case without the shaper. On the other hand, the inverse-shaper structure is able to cope with the disturbance and generate well damped response at the load-side. The achieved performance is better with the notch filter at the cost of higher actuator effort as in the previous case.

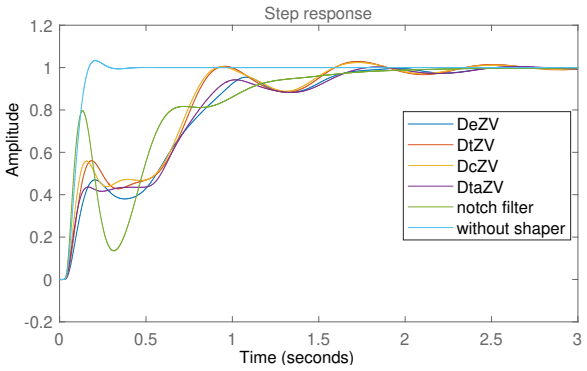

Fig. 8. Closed-loop actuator-side position response to step reference change, inverse shaper structure

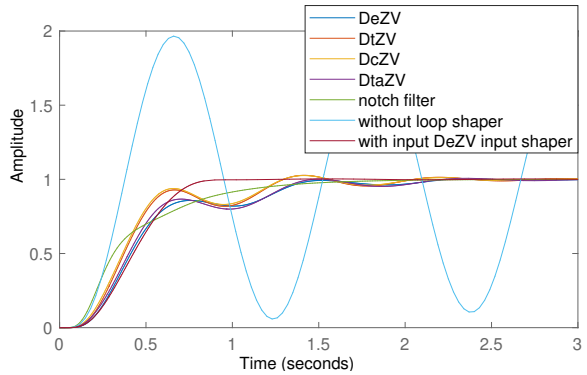

Fig. 9. Closed-loop load-side position response to step reference change, inverse shaper structure

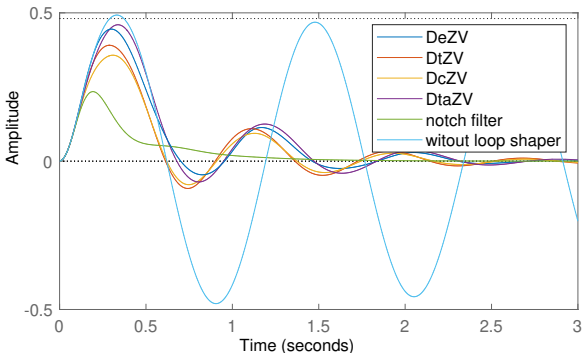

Fig. 10. Closed-loop load-side position response to step output disturbance change, inverse shaper structure

5. CONCLUSIONS

A systematic approach to design a controller for feedback loops with signal shapers was proposed and tested on a Gantry crane anti-sway problem. The proposed control design method is based on application of recently proposed H_∞ region approach. The method determines regions in the controller parameter space where the desired requirement on the robustness is satisfied. A crucial advantage of the method is that its applicability is not limited by the system order. Thus, it can be efficiently applied to infinite order time delay systems. Moreover, a complete set of

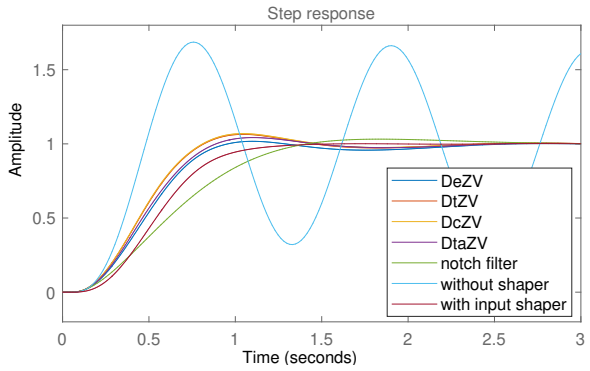

Fig. 11. Load-side response to step reference change, control-action shaper structure

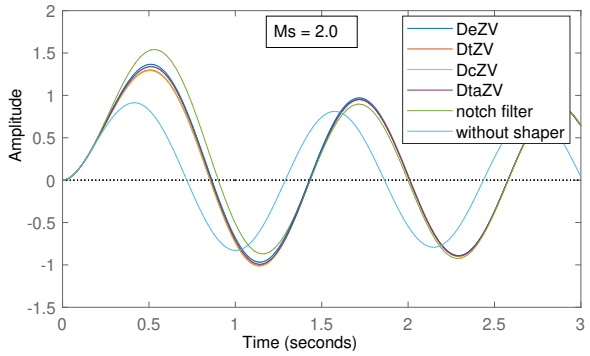

Fig. 12. Load-side position response to step output disturbance, control-action shaper

admissible controllers is derived directly in the parametric space from the robustness conditions.

For the Gantry crane application, four types of distributed delay shapers, proposed by Vyhlídal and Hromčík (2015) were tested. It is shown that the applicable parameter regions for which the desired robustness level is achieved are considerably smaller compared to the region for shaper free closed loop. Still, a reasonably fast and robust controller setting can be determined for all the considered cases. The performance of time delay shaper architectures is also compared with performance of architectures with conventional IIR single-mode notch-filter. Despite the design task is considerably simpler for this finite order option, the obtained responses confirm that time delay based signal shapers should be preferred due to ability to distribute the control actions with respect to oscillatory mode period.

6. ACKNOWLEDGEMENT

The first two authors were supported from the H2020 ECSEL JU project I-MECH under grant agreement Nr. 737453 and from ERDF under project Intecom No. CZ.02.1.01/0.0/0.0/17_048/0007267. The third author acknowledges support from the ESIF, EU Operational Programme Research, Development and Education, and from the Center of Advanced Aerospace Technology (CZ.02.1.01/0.0/0.0/16_019/0000826), Faculty of Mechanical Engineering, Czech Technical University in Prague

REFERENCES

Alikoç, B., Bušek, J., Vyhlídal, T., Hromčík, M., and Ergenç, A.F. (2017). Flexible mode compensation by inverse shaper in the loop with magnitude saturated actuators. *IFAC-PapersOnLine*, 50(1), 1251–1256.

Goubej, M. and Schlegel, M. (2019). PI plus repetitive control design: H-infinity regions approach. *22nd International Conference on Process Control*.

Hromčík, M. and Vyhlídal, T. (2017). Inverse feedback shapers for coupled multibody systems. *IEEE Transactions on Automatic Control*, 62(9), 4804–4810.

Huey, J.R. and Singhose, W. (2009). Trends in the stability properties of clss controllers: a root-locus analysis. *IEEE Trans. Contr. Syst. Techn.*, 18(5), 1044–1056.

Huey, J.R., Sorensen, K.L., and Singhose, W.E. (2008). Useful applications of closed-loop signal shaping controllers. *Control Engineering Practice*, 16(7), 836–846.

Hung, J.Y. (2003). Feedback control with posicast. *IEEE Transactions on industrial electronics*, 50(1), 94–99.

Pilbauer, D., Michiels, W., Bušek, J., Osta, D., and Vyhlídal, T. (2018). Control design and experimental validation for flexible multi-body systems precompensated by inverse shapers. *Systems & Control Letters*, 113, 93–100.

Pilbauer, D., Michiels, W., Vyhlídal, T., and Hromčík, M. (2017). Mixed-sensitivity design of a dynamic controller for systems pre-compensated by input shapers. *IFAC-PapersOnLine*, 50(1), 1304–1309.

Schlegel, M. and Medvecová, P. (2018). Design of PI controllers: H-infinity region approach. *15th IFAC Conference on Programmable devices and Embedded systems*.

Singer, N.C. and Seering, W.P. (1990). Preshaping command inputs to reduce system vibration. *J. of dyn. systems, measurement, and control*, 112(1), 76–82.

Singhose, W. (2009). Command shaping for flexible systems: A review of the first 50 years. *International J. of Precision Eng. and Manufacturing*, 10(4), 153–168.

Singhose, W., Kim, D., and Kenison, M. (2008). Input shaping control of double-pendulum bridge crane oscillations. *J. Dyn. Systems, Measurement, and Control*, 130(3), 034504.

Singhose, W., Seering, W., and Singer, N. (1994). Residual vibration reduction using vector diagrams to generate shaped inputs. *J. of Mech. Design*, 116(2), 654–659.

Smith, O.J. (1958). Feedback control systems. *New York: McGraw-Hill Book Co., Inc.,*, pp. 331–345.

Staehlin, U. and Singh, T. (2003). Design of closed-loop input shaping controllers. In *Proc. of the 2003 American Control Conference, 2003.*, volume 6, 5167–5172. IEEE.

Vaughan, J., Kim, D., and Singhose, W. (2010). Control of tower cranes with double-pendulum payload dynamics. *IEEE Trans. Contr. Syst. Techn.*, 18(6), 1345–1358.

Vyhlídal, T. and Hromčík, M. (2015). Parameterization of input shapers with delays of various distribution. *Automatica*, 59, 256–263.

Vyhlídal, T., Hromčík, M., Kučera, V., and Anderle, M. (2016). On feedback architectures with zero-vibration signal shapers. *IEEE Trans. on Automatic control*, 61(8), 2049–2064.

Vyhlídal, T., Kučera, V., and Hromčík, M. (2013). Signal shaper with a distributed delay: Spectral analysis and design. *Automatica*, 49(11), 3484–3489.